

## Growth, Mechanical, Electrical, Optical, and Thermal properties of $\gamma$ - Glycine crystal Grown using the Aqueous Solution of $\alpha$ -Glycine and Guanidine Hydrochloride

D.Arul Asir Abraham<sup>1\*</sup>, U.Sankar<sup>2</sup>, S.Perumal<sup>3</sup>, P.Selvarajan<sup>4</sup>

<sup>1</sup>Department of Physics, St. John's College, Palayamkottai-627002, Tamil Nadu, India.

<sup>2</sup>Department of Physics, Sri K.G.S Arts College, Srivaikuntam-628601, Tamil Nadu, India.

<sup>3</sup>Physics Research Centre, S.T.Hindu College, Nagercoil-629003, Tamil Nadu, India.

<sup>4</sup>Department of Physics, Aditanar College of Arts and Science, Tiruchendur-628216, India.

**Abstract:** An organic nonlinear optical single crystal of gamma glycine (GGLY) has been grown by slow evaporation of the saturated solution at room temperature. Single crystal of gamma glycine (GGLY), an organic nonlinear optical (NLO) material, has been grown by slow solvent evaporation technique. Good optical quality single crystals with dimension up to  $32 \times 31 \times 7 \text{ mm}^3$  are obtained. The crystals are characterized by optical absorption spectrum, FTIR and X-ray diffraction studies. The dielectric response of the sample is studied as a function of frequency and temperature. The mechanical, photoconductivity and ac/dc behavior and Differential thermal analysis (DTA) and thermo gravimetric analysis (TGA) study of the grown crystals are also investigated.

**Key words:** NLO materials; Crystal growth; Dielectric measurement; Conductivity; Mechanical and thermal properties.

### Introduction

The demand for NLO materials is always high due to its practical applications in optical modulation, switching and other signal processing devices. The research on organic and semi-organic crystals was started in 1980s. Organic materials offer good optical response time, non-resonant susceptibility, second harmonic generation and high phase-conjugate reflectivity [1] materials.

Amino acids and their complexes belong to a family of organic materials that have been considered for photonic applications [2]. Amino acids are essential materials for NLO applications. The importance of amino acids in NLO applications is due to the fact that all the amino acids have chiral symmetry and crystallize in non Centro-symmetric space groups. Out of 20 amino acids glycine is the simplest of all. The Glycine family crystals have been subjected to extensive research by several researches for their efficient NLO properties [3-6]. Glycine is the only protein forming amino acid and is optically inactive too. It exists as dipolar ions in which the carboxyl group is present as a carboxyl ate ion and the amino group as an ammonium ion. Its high melting point is due to its dipolar nature. Under different conditions, glycine crystallizes in 3 kinds of polymorphs with different thermal stabilities [7]. Also  $\alpha$ ,  $\beta$  and  $\gamma$  glycine exhibit different characteristics. Both  $\alpha$  and  $\beta$  forms are crystalline in centrosymmetric space

group P2<sub>1</sub>/c that is not feasible for optical second harmonic generation [8-9]. But  $\gamma$  glycine crystallizes in non centrosymmetric space group P3<sub>1</sub> & P3<sub>2</sub>, enabling itself ideal for piezo electric and NLO applications. Due to the presence of chromophores namely amino groups, carboxyl group,  $\gamma$  glycine finds itself absolutely transparent in the U-V visible region.

Many researchers reported that single crystals of GGLY (gamma glycine) can be grown from aqueous solutions of glycine which can be acidic as well as basic [10-12]. The growth of single crystals of Gamma glycine from aqueous solution incorporated with sodium chloride (NaCl) has been reported recently by Srinivasan and Arumugam employing slow solvent evaporation technique [13]. Ambujam et al [14] and Ramachandran et al [15] have successfully crystallized GGLY (Gamma glycine) via gel technique. A scaled quantum mechanical force field calculations on the Gamma Crystal polymorph have confirmed the effect of hydrogen bond stretching in vibrational analysis. Gamma Glycine is actually grown by many conventional methods like slow cooling, slow evaporation as well as gel method. Though there are numerous reports on this title compound wherein mixed solvents like water with sodium acetate, sodium hydroxide, ammonium sulphate, ammonium hydroxide, potassium chloride, lithium bromide, lithium acetate etc are used, still the indispensable characteristics of gamma glycine urges the researches to implant deeper studies on its properties. Bharaniraj et al have been reported the growth of gamma glycine from the aqueous solutions of alpha glycine and sodium acetate with deionised water. The present article also addresses the growth of Gamma glycine crystals in the presence of the aqueous solution of  $\alpha$ -Glycine and guanidine hydrochloride. The crystals of Gamma glycine grown with Guanidine Hydrochloride are characterized by single crystal and powder XRD, FT-IR, NLO test, optical, micro hardness, dielectric, Electrical conductivity, photoconductivity study and thermo gravimetric analysis (TGA) studies.

## Materials and Methods

### 2. Experimental procedure

#### 2.1 Synthesis

The single crystals of Gamma Glycine (GGLY) crystals were grown by slow evaporation method at ambient room temperature. The commercially available analar grade Glycine (99.5%) and Guanidine hydrochloride mixture of 1:1 molar ratio was dissolved in de-ionised water and was stirred at 50 °C then the solution was filtered in room temperature (30 °C). Colourless transparent crystals of the title compound were formed by slow evaporation technique after four to nine weeks.

#### 2.2 Solubility determination

The growth rate of a crystal depends on its solubility and growth temperature. Solubility of a material governs the amount of material, which is available for the growth and hence defines the total size limit. The solubility curve of Gamma Glycine (Glycine and Guanidine Hydrochloride) was determined by dissolving the synthesized product in Millipore water in an airtight container kept in a constant temperature bath, the content was continuously stirred for 1-2 hours. After attaining the saturation, the equilibrium concentration of the solute was estimated gravimetrically. The same process was repeated for different temperatures (30, 35, 40, 45, 50 and 55 °C). The variation of solubility with temperature Fig. 1 indicates that  $\gamma$ -glycine with Guanidine hydrochloride have high positive solubility-temperature co-efficient values.

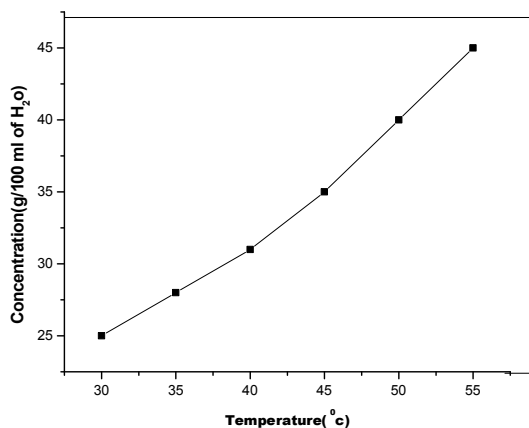


**Fig. 1 Solubility curve of GGLY(Glycine with Guanidine hydrochloride)**

### 2.3 Crystal Growth

The synthesized salt of Gamma Glycine (GGLY) is purified by repeated crystallization and saturated solution is prepared in accordance with the solubility. The optimized pH is measured to be 5.5 respectively. Saturated aqueous solution of GGLY(Glycine and Guanidine Hydrochloride)1:1 is taken in a crystallizing vessel with perforated covers and placed in a constant temperature bath. Seed crystals are harvested within few weeks. A suitable seed crystal is selected from the harvested crystals. A saturated solution is prepared and the seed crystal is hung inside the solution that is optimally closed for controlled evaporation. By slow evaporation of the solvent, Gamma Glycine (GGLY) single crystal of size  $32 \times 31 \times 7 \text{ mm}^3$  is grown in a period of 30-60 days. The resulting crystals are of colorless needles. The grown crystals are stable, do not decompose in air and non-hygroscopic in nature. Fig .2 shows the photograph of the as grown crystals of Gamma Glycine (GGLY). An important observation during the growth of GGLY is the absence of any kind of microbial contamination during the growth period even when the solution was kept for nearly 1 -2 months.



**Fig. 2 Photograph of GGLY Crystal grown from Guanidine hydrochloride**

### 2.4 Characterization

The grown crystal of GGLY was confirmed by single crystal X-ray diffraction analysis. Single crystal XRD data was collected by ENRAF NONIUS CAD4-F single crystal X-ray diffractometer with MoK $\alpha$  ( $\lambda=0.71073 \text{ \AA}$ ) radiation. The grown crystals of GGLY were confirmed by powder XRD analysis. In this system, a fine focus (0.4 x 8 mm; 2 kW Mo) X-ray source energized by a well-stabilized Philips X-ray generator (PW 1743) was employed. The FT-IR spectrum was recorded using BRUKER IFS-66V FT-IR spectrometer with KBr pellet technique for the range  $4000 - 400 \text{ cm}^{-1}$ . The linear optical properties of the crystals were examined between 200 and 2000 nm using the VARIAN CARY 5E UV-Vis-NIR spectrophotometer. The powder SHG measurement was done using

Nd:YAG laser fundamental ( $\lambda = 1064$  nm) radiation. In this work, HMV SHIMADZU microhardness tester, fitted with diamond Vickers pyramidal indenter was used. The static indentations were made at room temperature with a constant indentation time of 20 seconds for all indentations. Indentations were made by varying the loads from 10 to 50 g; above this load micro cracks are observed. Good quality single crystals of GGLY grown (Glycine added with Guanidine hydrochloride) were selected for dielectric measurements. Silver paint was applied on opposite faces of planes of the crystal grown with Guanidine Hydrochloride, respectively, to make a capacitor with the crystal medium. The dielectric constant ( $\epsilon_r$ ) and dielectric loss ( $\tan \delta$ ) of the samples were determined by measuring the capacitance and dissipation factor as a function of frequency (100 Hz-5 MHz) and temperature ( $T = 308$ – $368$  K). Using a HIOKI-3532 LCR HITESTER the ac conductivity study was taken.

## Results and Discussion

### 3.1 Structural studies

#### 3.1.1 Single crystal XRD analysis

The structure of GGLY (Gamma Glycine) was solved by the direct method and refined by the full matrix least-squares fit technique employing the SHELXL program. It is observed that GGLY crystal crystallizes in the Hexagonal system with space group  $P_63_2$ . The lattice parameters are  $a = 7.011$  Å,  $b = 7.011$  Å,  $c = 5.469$  Å and volume  $V = 232.83$  Å<sup>3</sup>. The single crystal XRD data is obtained in the present work coincides with the previously reported work.

#### 3.1.2 Powder XRD analysis

The Powder XRD pattern of the grown crystals was recorded using D8 Advanced Bruker Powder X-ray Diffractometer. The positions of the peaks are found to be matching with the literature. Fig. 3 depicts the powder XRD pattern of the  $\gamma$  glycine crystals.

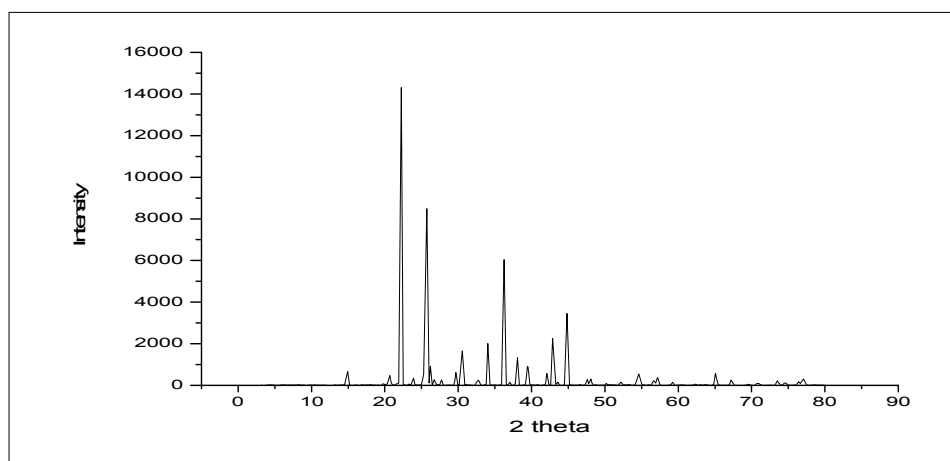
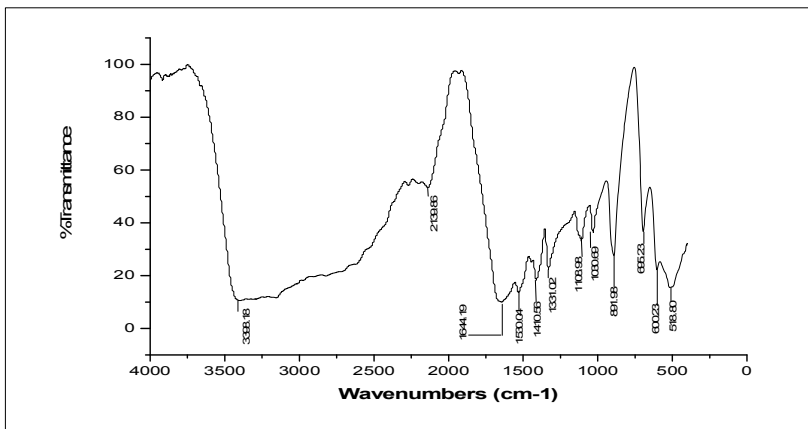


Fig. 3 Powder XRD data of GGLY grown from ( Guanidine Hydrochloride)

#### 3.1.3 FT-IR Spectroscopic Studies

This analysis was accomplished to identify the functional groups present in the grown crystal. For this, an Alpha-T/Bruker Spectrometer was used in the frequency range  $400 - 4000$  cm<sup>-1</sup>. The sample used was in pellet form in KBr phase. The FT-IR spectrum is depicted in the Fig. 4 which was found to be matching with the previous literature.



**Fig. 4 FT-IR Spectrum for GGLY grown from Guanidine Hydrochloride**

**Table 1 FT-IR spectral assignments for GGLY**

Wave number	Assignments
3398.10	N-H asymmetric stretch
2139.86	Combination and overtone bands
1644.19	-COO <sup>-</sup> asymmetric stretch
1530.14	NH <sub>3</sub> <sup>+</sup> symmetric bending
1410.56	-CH <sub>2</sub> bend
1331.02	-COO <sup>-</sup> symmetric stretch
1108.98	-CH <sub>2</sub> wag
1030.69	NH <sub>3</sub> <sup>+</sup> rock
928.70	-CH <sub>2</sub> rock
891.98	-CCN symmetric stretching
695.23	-COO <sup>-</sup> bend
602.23	NH <sub>3</sub> <sup>+</sup> torsion
518.80	-COO <sup>-</sup> rock

### 3.2 Optical properties

#### 3.2.1 UV-VIS Spectroscopy study

Nonlinear optical single crystals are mainly used in optical applications. The optical absorption range and the cut-off wavelength are the most important optical parameters for laser frequency applications. Fig. 5 represents the optical absorption spectrum of GGLY. The UV cut-off wavelength of the sample is found to be at 220 nm and the absorption is very less in the entire visible region and part of IR region. The optical band gap is obtained by plotting the graph between  $h\nu$  and  $(\alpha h\nu)^2$  (Fig. 6). From the graph, the optical energy gap of GGLY is determined as 3.25 eV.

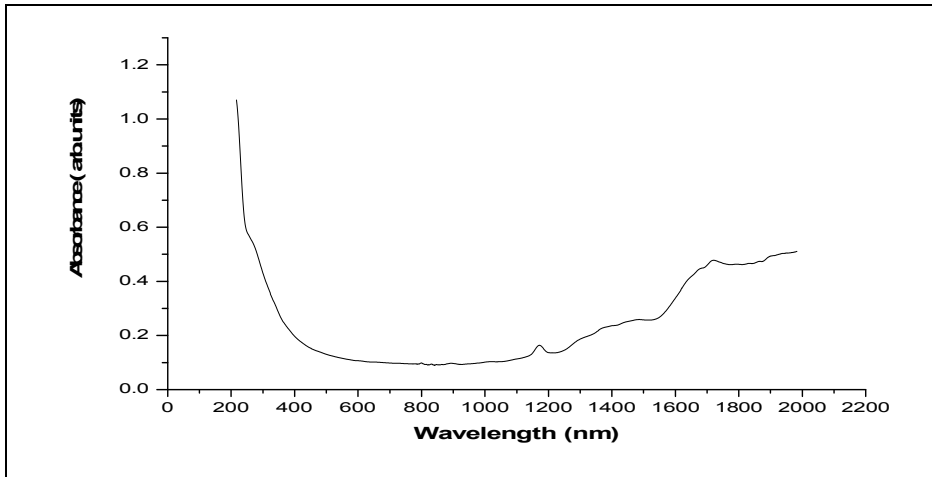


Fig. 5 Optical absorption spectrum of Gamma Glycine crystal

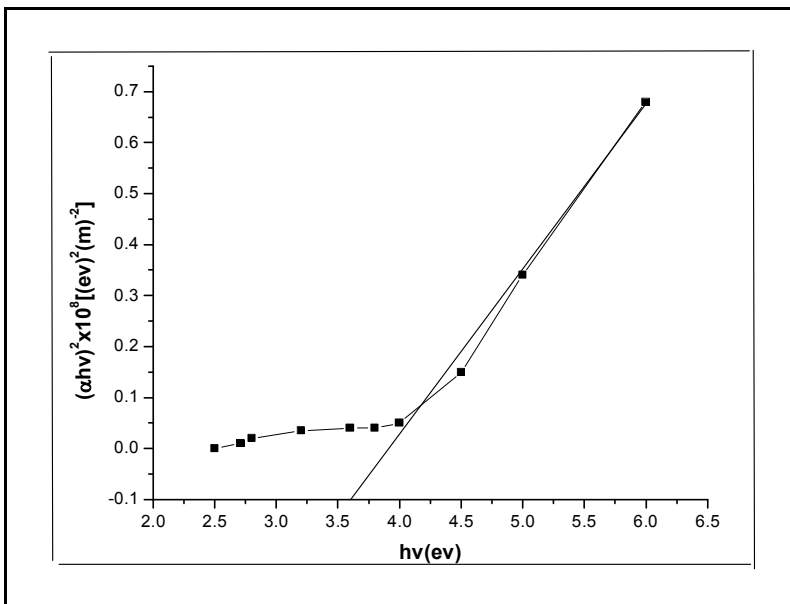
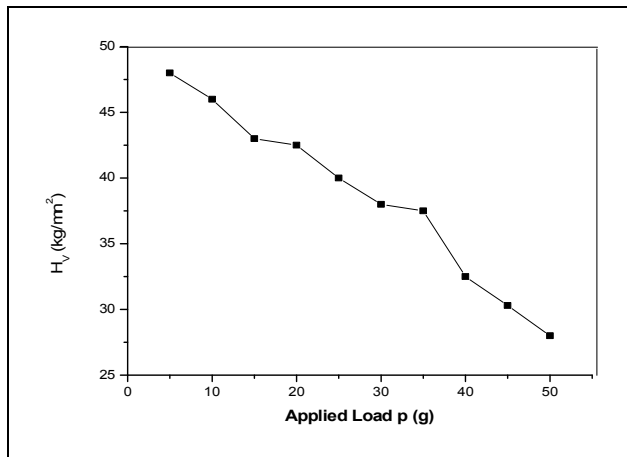


Fig. 6 Tauc's plot of Gamma Glycine

### 3.2.2 NLO studies

Kurtz and Perry powder SHG test was carried out on grown GGLY single crystals to study the NLO properties. The second harmonic generation (SHG) test on the GGLY crystal is performed by Kurtz powder SHG method [16]. The fundamental beam of Nd: YAG laser with 1064 nm wavelength, pulse duration of 8 ns and 10 Hz repetition rate is focused onto the powdered sample of GGLY and KDP. When the input pulse of 3.2 mJ is passed through the sample and KDP, output signals of 55 and 112 mV are obtained from GGLY and KDP respectively. It is observed that the NLO efficiency of GGLY is two times more that of KDP crystal.



**Fig. 7 Variation of Vickers Hardness Number with the applied load for GGLY**

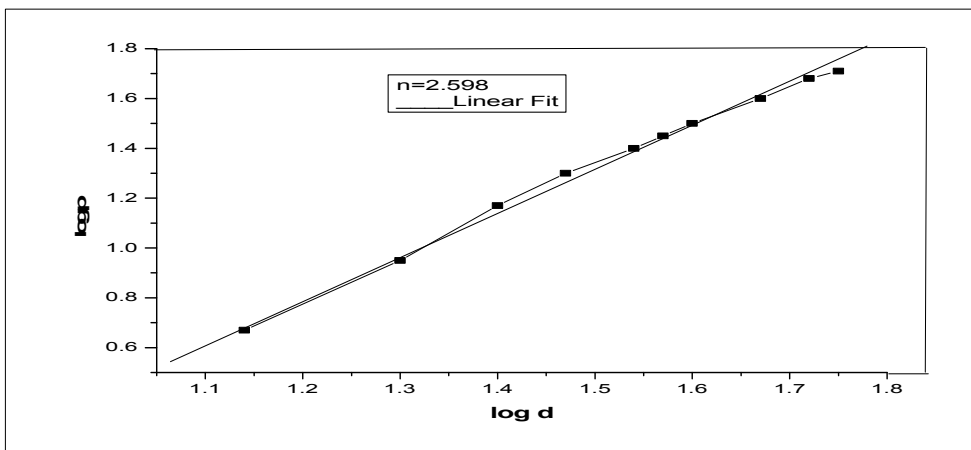


**Fig. 8 Plot of log d versus log p for Gamma Glycine**

### 3.3 Microhardness studies

A plot between the hardness number and the applied load is depicted in Fig. 7. It is evident from the figure that the Vickers Hardness number ( $H_V$ ) decreases with applied load ( $p$ ). This indicates that the crystal exhibits normal indentation size effect behavior (ISE). A plot drawn between  $\log p$  and  $\log d$  is shown in Fig. 8. It supports normal ISE behavior of GGLY single crystal [17]. From the graph the work hardening coefficient ( $n$ ) is calculated using linear fit method and is found to be 2.598.

### 3.4 Electrical properties

#### 3.4.1 Dielectric studies

Fig. 9 shows the plot of dielectric constant ( $\epsilon_r$ ) versus log frequency for 308, 328 and 348 K. It is seen that the value of dielectric constant is high in the lower frequency region for all the temperatures and then it decreases with increase in frequency up to 10 kHz. The high value of dielectric constant at low frequency is attributed to space charge polarization due to charged lattice defects. Beyond 10 kHz, it is almost constant and is saturated at higher frequencies [18]. A graph is drawn between dielectric loss and log frequency for various temperatures (308, 328 and 348 K) and is shown in Fig. 10. The low value of dielectric loss at high frequency suggests that the GGLY crystals possess good optical quality [19]. This parameter is of vital importance for nonlinear optical materials in their applications. In Fig. 11 and 12 the temperature dependence of dielectric constant and dielectric loss for various frequencies are shown.

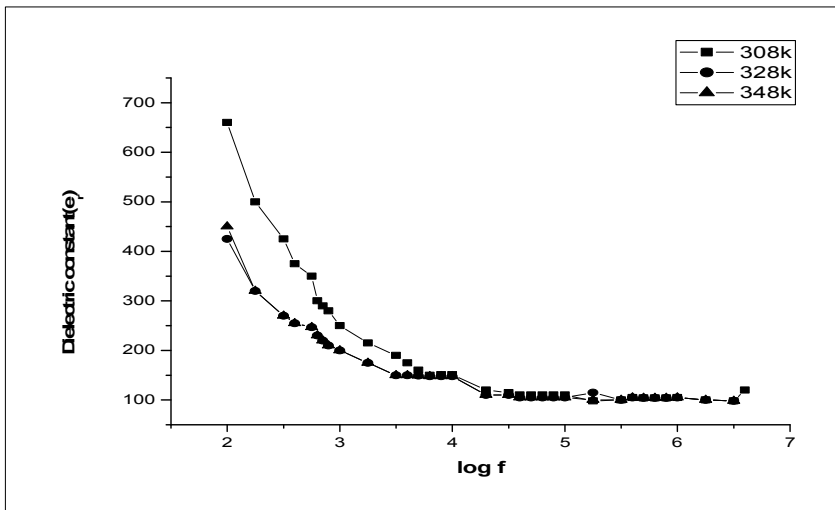


Fig. 9 Variation of dielectric constant with log frequency for Gamma Glycine

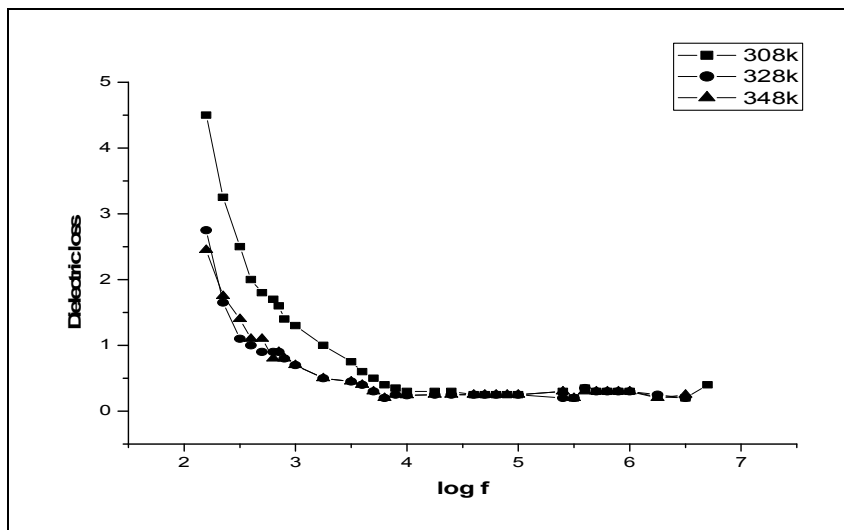


Fig 10. Variation of dielectric loss with log frequency for Gamma Glycine

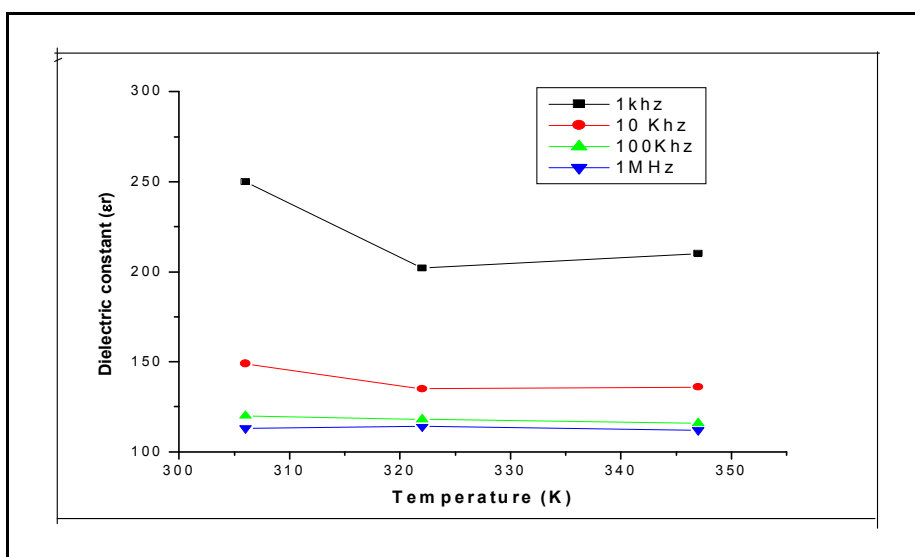


Fig 11. Temperature dependence with dielectric constant for Gamma Glycine



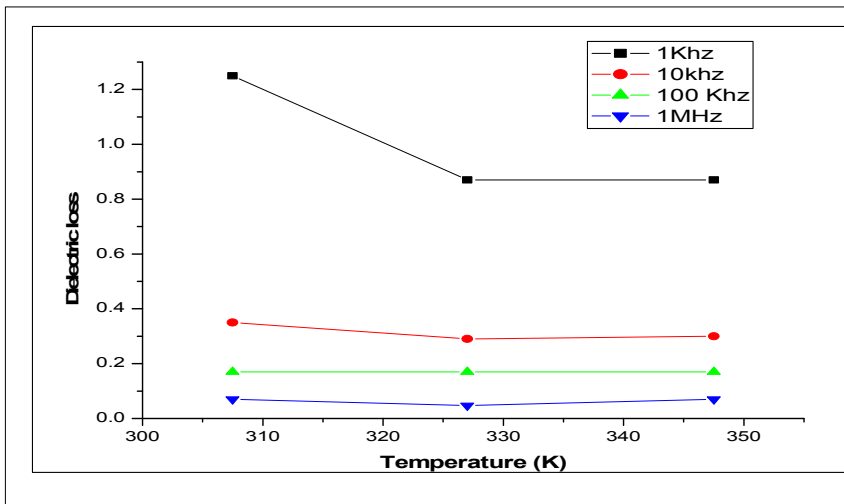


Fig. 12 Temperature dependence of dielectric loss for Gamma Glycine

### 3.4.2 *Ac* conductivity study

The *ac* conductivity measurements are taken using HIOKI 3532-50 LCR HITESTER in the frequency range 50 Hz to 5 MHz. In Fig.13 the sample is subjected to a temperature variation from 313 to 423 K. Temperature dependence of conductivity is shown. The Arrhenius plot of  $\sigma T$  versus  $1000/T$  is shown in Fig. 14. It is evident from the graph that the conductivity increases with the temperature. Accordingly the value of activation energy for ionic migration is estimated from the slope of the Arrhenius plot. The line of best fit for the plot of  $\log \sigma T$  versus  $1/T$  obeys Arrhenius relationship.

$$\sigma = \sigma_0 \exp (E_a/kT)$$

Where  $\sigma_0$  is the pre-exponent factor,  $E_a$  the activation energy for the conduction process and  $k$  is the Boltzmann constant. Therefore, the sample exhibits Arrhenius type conductivity behavior in the frequency range of investigation. The activation energy of GGLY for the conduction process, calculated from the plot is found to be 0.009 eV.

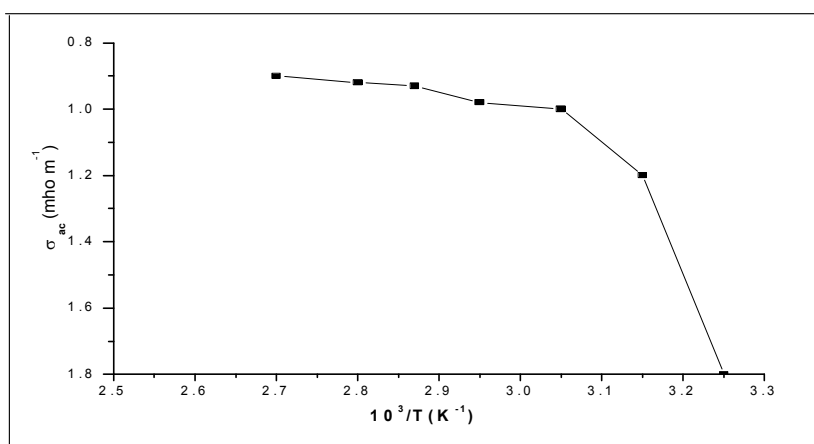
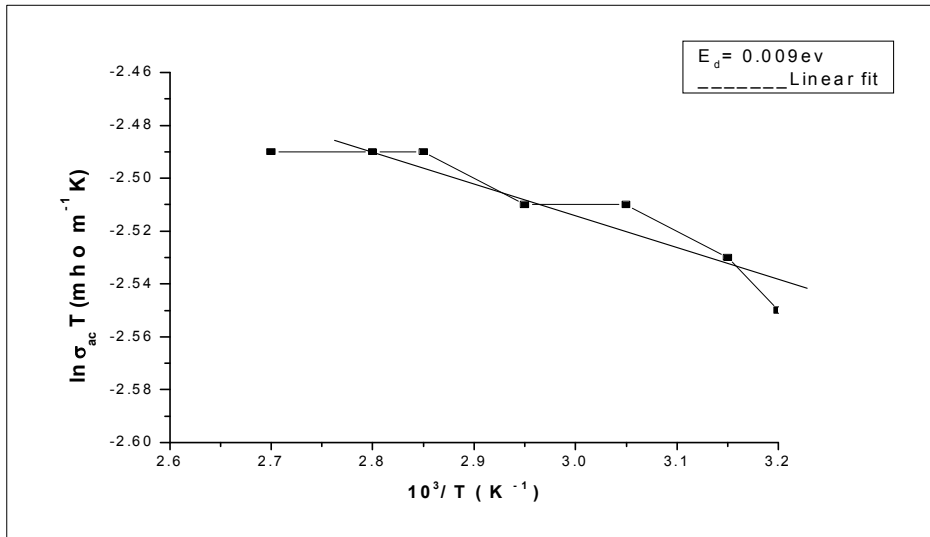


Fig. 13 Variation of *ac* conductivity with  $1000/T$  for Gamma Glycine



**Fig. 14** Plot of  $\ln(\sigma_{dc})T$  versus  $1000/T$  for Gamma Glycine

### 3.4.3 Dc conductivity studies

The *dc* electrical conductivity ( $\sigma_{dc}$ ) as a function of temperature is shown in Fig. 15. It is observed that conductivity increases with temperature indicating the temperature dependence activation energy ( $E_d$ ) which is a characteristic of small polaron hopping (SPH) conduction mechanism. The plot of  $\ln \sigma T$  versus  $1000/T$  is shown in Fig. 16. The logarithmic conductivity in the temperature range (313–423 K) exhibits almost linear dependence on reciprocal temperature i.e. thermally activated behavior. The SPH model is based on a strong coupling of electron with the lattice by a single phonon. According to this model the *dc* conductivity is given by

$$\sigma = \sigma_0 \exp(-E_d/kT)$$

Where  $\sigma_0$  is a pre exponential factor,  $E_d$  is the activation energy,  $k$  is Boltzmann constant and  $T$  is temperature in K. The activation energy calculated from the slope of the graph (Fig. 16) it is found to be 0.044 eV. The low value of activation energy and high value of electrical conductivity are similar to those of LAO, LAM and MAN [20-22]. This is in consistent with small polar on hopping theory [23] result.

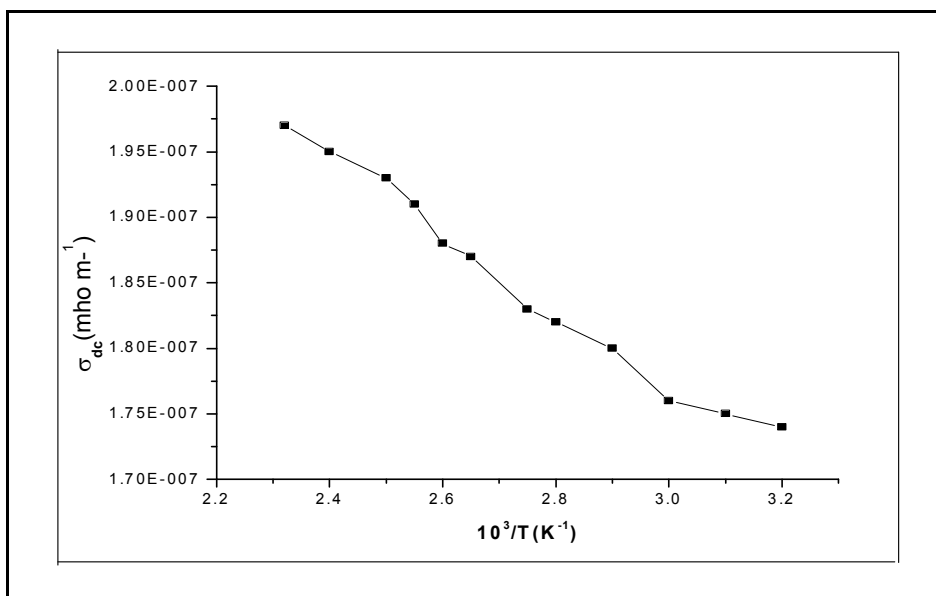


**Fig. 15** Variation of *dc* conductivity with  $1000/T$  for Gamma Glycine

### 3.5 Photoconductivity studies

Fig. 17 shows the plot of dark current and photo current against electric field. It is observed from the graph that both dark and photo currents increase linearly with the applied electric field, but the photo current is less than the dark current which is termed as negative photoconductivity[24]. The negative photoconductivity in a solid is due to the reduction in the number of charge carriers or their life time in the presence of radiation. The decrease in mobile charge carriers during negative photoconductivity can be explained by the Stockman model [25].The structure material containing molecular bonding for suitable conductivity analyzed in[26].

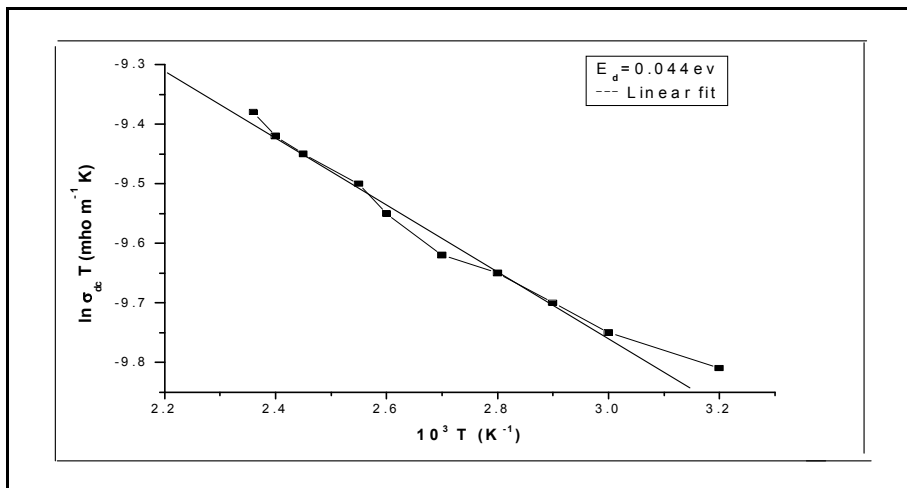


Fig. 16 Plot of  $\ln(\sigma_{dc})T$  versus  $1000/T$  for Gamma Glycine

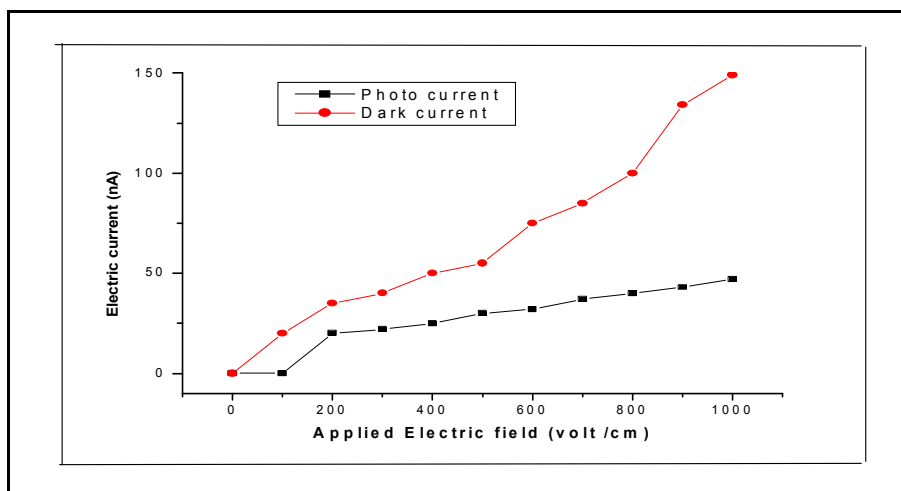
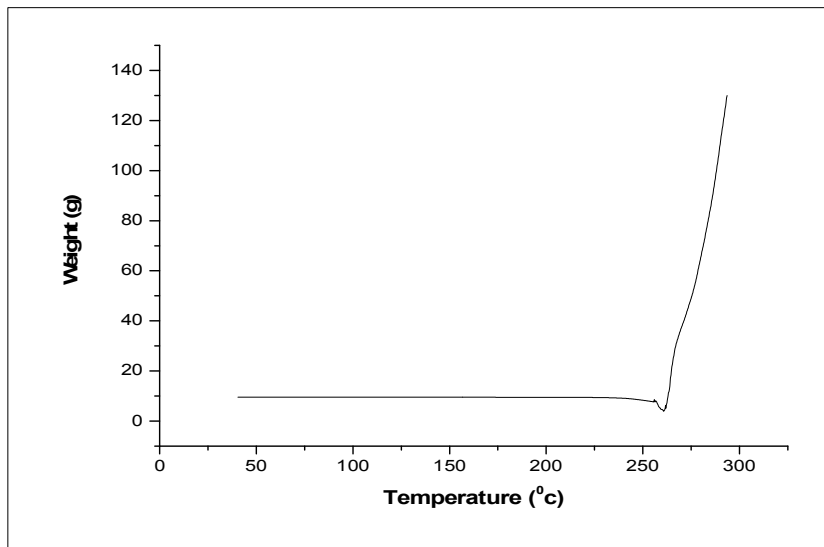


Fig. 17 Field dependent photoconductivity of Gamma Glycine

### 3.6 Thermal characterization

The TG / DTA studies were carried out simultaneously on the sample in the temperature range 37 – 310°C and the recorded thermal curves are displayed in figure 18. From the TG curves, it is noticed that there is a slight weight loss up to 220°C [27] for the sample and there is a maximum weight loss in the temperature range 260-270°C. Hence the sample is found to be thermally stable and suitable for device applications. From DTA curves it is observed that the sample has an endothermic peak at 276°C which corresponds to the decomposition point of the sample. In TGA/DTA curve the transition temperature at 240 °C, the gamma Glycine samples are due conversion  $\gamma$ -glycine into  $\alpha$ -glycine. The high melting point of the semi organic material when compared to the other crystals arises due to the strong bonding between the conjugation layers[28].The sample crystal thermally stable for designing the NLO applications.



**Fig. 18. DSC thermogram of Gamma glycine single crystal**

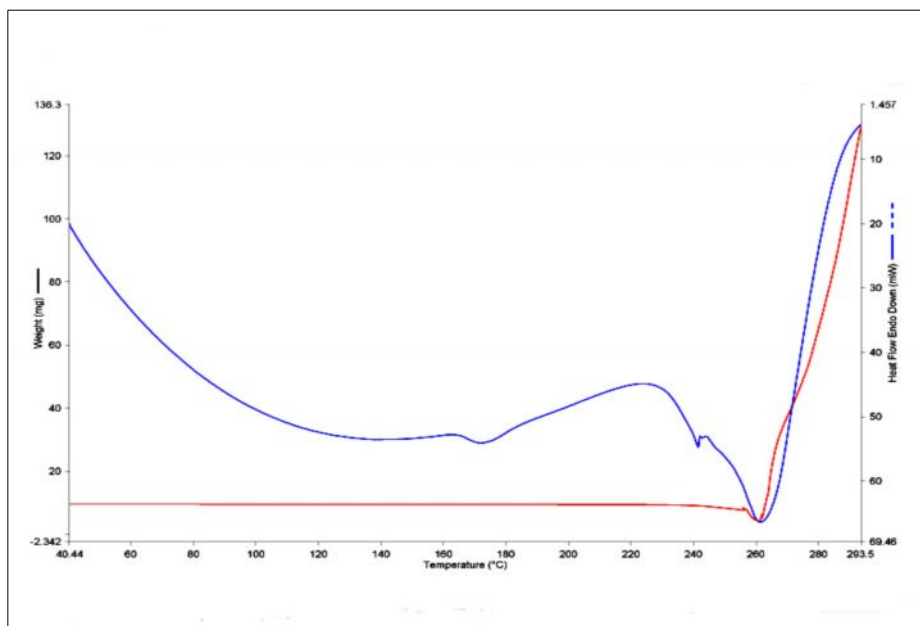


**Fig. 19. TG-DTA curve of Gamma glycine crystal.**

## Conclusion

The Glycine and Guanidine Hydrochloride compound of GGLY was successfully synthesized and the single crystals have been grown by solution growth technique. Its cell parameters have been determined by the single crystal XRD and powder XRD analysis. The presence of functional groups in gamma glycine has been identified from the FTIR analysis. Optical absorption study reveals the absorption edge at 220 nm. The phase matching natures of the grown crystals have been confirmed by Kurtz and Perry powder method. The micro hardness measurements prove that gamma glycine belongs to the soft category of materials. The activation energy is determined from the plots of *ac/dc* conductivity. The negative photo conducting nature of the sample is confirmed by photo conductivity study. The thermo characteristic study confirm the crystal is stable and is suitable for device applications.

## Acknowledgement

The authors thank SAIF, IIT-Madras and St Joseph's college, Trichy for their help and support.

## References

1. Prasad PN, Williams DJ, Introduction to Nonlinear Optical Effects in Molecules and Polymers, Wiley-InterScience, New York, 1991.
2. Narayana Moolya B, Jayarama A, Sureshkumar M.R, Dharmaparakash S.M, J. Cryst. Growth, 2005, 280, 581.
3. Albert L. Lehninger, Principles of Biochemistry, CBS Publishers, New Delhi, 1984.
4. Marsh RE, Acta Crystallogr., 1958, 11, 654.
5. Itaka Y, Acta. Crystallogr., 1960,13, 35.
6. Itaka Y, Acta. Crystallogr., 1961,14, 1.
7. Xia Y, Jie L, Xiu-Juan W, Chi-Bun C (2008). Effect of sodium chloride on the nucleation and polymorphic transformation of glycine. J. Cryst. Growth 310:604-611.
8. Akihiko Ito, Maiko Yamanobe-Hada, Hitoshi Shindo, J. Crystal Growth, 2005, 275, 1691.
9. Narayan Bhat MK, Dharmaparakash SM, J. Crystal Growth, 2002, 236, 376.
10. Narayan Bhat MK, Dharmaparakash SM, J. Crystal Growth, 2002, 242, 245.
11. Moolaya BN, Jayarama A, Sureshkumar MR, Dharmaparakash SM, J. Crystal Growth, 2005, 280, 581.
12. Jan Baran, Henryk Ratajezak, Spectrochimica Acta Part A, 2005 61, 1611
13. Srinivasan K, Arumugham J, Optic.Materials, 2007, 30, 40.
14. Ambujam. K, Selvakumar S, Prem Anand D, Mohamed G, Sagayaraj P, Cryst. Res. Technol., 2006, 41, 671.
15. Ramachandran E, Baskaran K, Natarajan S, Cryst. Res. Technol., 2007, 42, 73.
16. Kurtz SK, Perry T.T, J. Appl. Phys., 1968,39, 3798 3813.
17. Onitsch E.M., 'The present status of testing the hardness of materials', Mikroskopie, 1956, 95, 12-14.
18. Smyth CP, (1965) Dielectric behavior and structure, McGraw Hill, Newyork.
19. Balarew CP, Duhlew R, J. Solid State Chem., 1984, 55, 1-10.
20. Vimalan M, Ramanand A, Sagayaraj P, Crys. Res. Technol., 2007, 42, 1091- 1096.
21. Vimalan M, Cyrac Peter A, Rajesh Kumar T, Jayasekaran R, Packiam Julius J, Sagayaraj P, Arch. Phy. Res., 2010, 1 (2): 94-102.
22. Vimalan M, Helan Flora X, Tamilselvan S, Jeyasekaran R, Sagayaraj P, Mahadevan C.K, Arch. Phy. Res., 2010, 1 (3):44-53
23. Mott BW, (1956) Microindentation Hardness testing, Butterworths, London.
24. Bube RH, (1981), Photoconductivity of Solids, Wiley Interscience, New York.
25. Joshi VN, (1990), 'Photoconductivity', Marcel Dekker, New York.
26. D.Arul Asir Abraham et al/Int.J.Chemtech Res.2015,8(1),pp 105-110.
27. G.L.Perlovich,L.K,Hansen,A.Baucer-Brand ,J.Therm. Anal.Calorimetry 66(2001) 699.
28. E.Ramachandran, K.Baskaran, S.Natarajan. Crys.Technol. 42(2007)73.

\*\*\*\*\*